Potential ^{18}F-labeled biomarkers for epidermal growth factor receptor tyrosine kinase

Thomas A. Bonasera[a], Giuseppina Ortu[a,b], Yulia Rozen[a], Roman Krais[a], Nanette M.T. Freedman[c], Roland Chisin[a], Aviv Gazit[d], Alexander Levitzki[b], Eyal Mishani[a,*]

[a]*Hebrew University, Hadassah University Hospital Campus, Department of Medical Biophysics and Nuclear Medicine, IL-91120, Jerusalem, Israel*
[b]*Hebrew University, Givat Ram Campus, Department of Biological Chemistry, Institute of Life Sciences, IL-91904, Jerusalem, Israel*
[c]*Hadassah University Hospital Campus, Department of Medical Biophysics and Nuclear Medicine, IL-91120, Jerusalem, Israel*
[d]*Hebrew University, Givat Ram Campus, Department of Organic Chemistry, Institute of Chemistry, IL-91904, Jerusalem, Israel*

Abstract

As PET candidate tracers for EGFr-TK, five 4-(anilino)quinazoline derivatives, each fluorinated in the aniline moiety, were prepared. Each was tested in vitro for inhibition of EGFr autophosphorylation in A431 cell line. The leading compounds were then radiolabeled with ^{18}F and cell binding experiments, biodistribution and PET studies in A431 tumor-bearing mice were performed. Metabolic studies were carried out in a mice control group. From our results, we concluded that while in vitro experiments indicates efficacy of 4-(anilino)quinazoline compounds, kinetic factors and rapid blood clearance make them unsuitable as tracers for nuclear medicine imaging of EGFr-TK. © 2001 Elsevier Science Inc. All rights reserved.

Keywords: EGFr; Tyrosine kinase; Quinazoline; Biodistribution; Fluorine-18; PET

1. Introduction

Positron emission tomography (PET), a nuclear medicine imaging technology which allows the three-dimensional, quantitative determination of the distribution of radioactivity within the human body, is becoming an increasingly important tool for the measurement of physiological, biochemical, and pharmacological function at a molecular level, both in healthy and pathological states. PET allows accurate measurement of radioactivity concentration in small volume elements in vivo as well as the ability to follow tracer kinetics. PET requires the administration to the subject of a molecule labeled with a positron-emitting nuclide such as ^{15}O, ^{13}N, ^{11}C and ^{18}F, which have half-lives of 2.037, 9.965, 20.39 and 109.8 min, respectively.

Epidermal growth factor receptor (EGFr) is often over expressed in cancer, and is thus a therapeutic target in the management of this multifaceted disease. Functionally, EGFr consists of an outer membrane EGF binding site and an inner membrane tyrosine kinase portion where, via the conversion of ATP to ADP, tyrosine residues either on EGFr itself or on intracellular proteins are phosphorylated, activating the respective protein. A suitable radiotracer that binds EGFr would allow, through a nuclear medicine imaging technique such as PET, the mapping and quantification of this receptor-kinase. One potential application is differential diagnosis of patients having tumors with high EGFr expression from those having tumors with low EGFr expression. High expressers would be candidates for EGFr-directed therapy, while low expressers would not.

Several markers have been described for the outer membrane portion of EGFr. In a clinical trial, ^{99m}Tc ($t_{1/2}$ = 6.01 h), used extensively in non-PET nuclear medicine imaging, was used to label a monoclonal antibody that binds EGFr [22]. Patients having tumors of epithelial origin were imaged successfully with this tracer. Indium-111 ($t_{1/2}$ = 67.3 h), another extensively used non-PET radionuclide, was used by at least two groups to label EGFr-binding antibodies for use in conventional nuclear medicine imaging [7,12]. EGF itself and certain derivatives have been labeled for nuclear medicine imaging with gamma emitting nuclides

* Corresponding author. Tel.: 972-2-6777931; fax: 972-2-6421203.
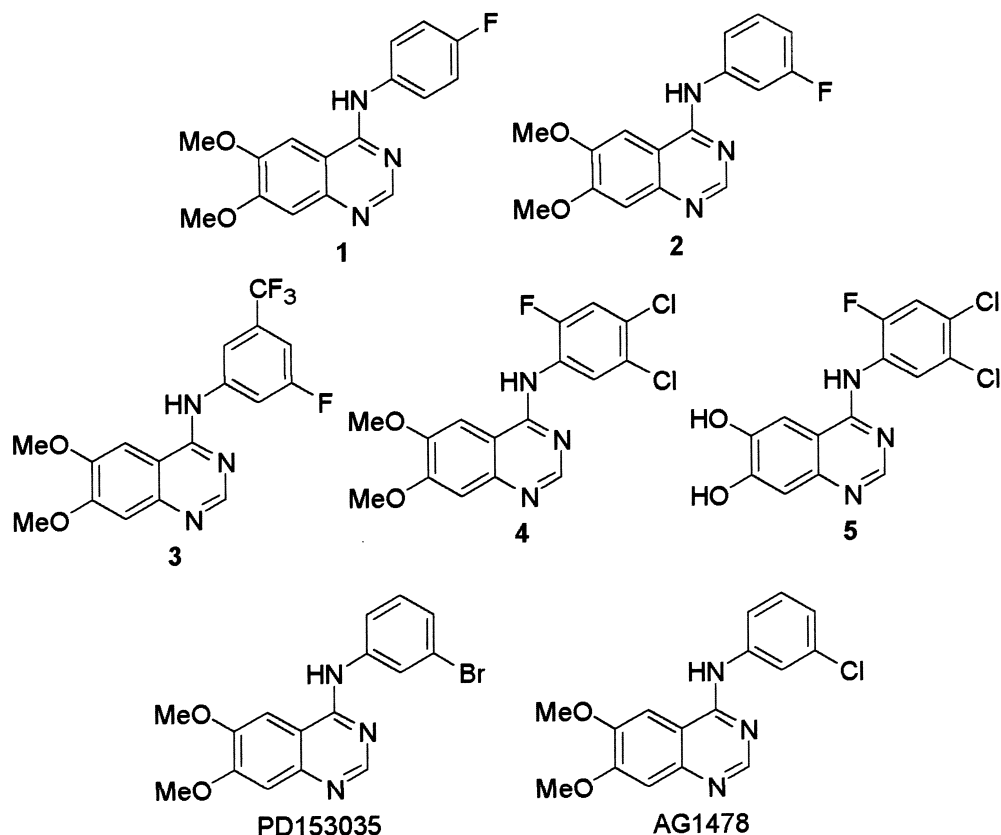*E-mail address:* mishani@md2.huji.ac.il (E. Mishani).

Fig. 1.

^{99m}Tc, [5] ^{111}In [15] and ^{131}I [27] ($t_{1/2}$ = 192 h) and the positron-emitting nuclide ^{76}Br ($t_{1/2}$ = 16.2 h) [28].

4-(Anilino)- and 4-[(phenylmethyl)amino]quinazolines have been shown to inhibit potently and selectively EGFr kinase activity by binding reversibly to the inner membrane ATP binding domain on EGFr, the prototype for such compounds being the small-molecules PD153035 [10,14] and AG1478 [11,16] (see Fig. 1). Appropriately labeled analogs of these compounds would therefore be candidates for nuclear medicine imaging of EGFr. A preliminary report of the synthesis of two radioiodinated (^{123}I ($t_{1/2}$ = 13.3 h) and ^{125}I ($t_{1/2}$ = 59.4 d), both non-PET radionuclides) analogs of PD153035 indicated specific binding in vitro in EGFr-TK-rich MDA-486 cells [20]. The same group also reported the labeling of PD153035 itself. In this case, PD153035 was labeled specifically with ^{11}C in the 7-methoxy position. Biodistribution experiments were performed in normal mice, but uptake specificity could not be demonstrated as administration of an enzyme-blocking dose of PD153035 caused an increase in tracer uptake in the tissues studied [21]. The same abstract reported the labeling of the 7-(2-fluoroethoxy) PD153035 analog with ^{18}F, but no biological experiments with this tracer were described. In the most complete report to date, ^{11}C-labeled (nonspecifically in either the 6- or 7-methoxy position) PD153035 was evaluated using PET in rats implanted with EGFr-rich human neuroblastoma SH-SY5Y xenografts [9]. While these studies included quantitative PET image analysis of tracer tissue kinetics, specific uptake was not demonstrated in a blocking study. Further, peak tumor uptake of only about 0.3% injected tracer dose per mL tissue was observed around 7 min, a time at which, in no tumor bearing animals, the gastrointestinal tract and the liver had 2–2.5 times more radioactivity.

Another approach to small molecules as EGFr PET tracers utilizes 4-(anilino)- and 4-[(phenylmethyl)amino]quinazolines labeled with ^{18}F on the aniline or phenyl ring [17, 26]. We hypothesized that changing the labeling position and the radionuclide could lead to a better results than those published. Considering that the demonstration of a clinically useful small molecule tracer for EGFr-TK has not been reported, we thought that it would be worthwhile developing such a radiopharmaceutical. In this report we describe the non-radioactive and radioactive syntheses and biological evaluation of 4-(fluoroanilino)quinazoline derivatives as potential PET biomarkers of EGFr expression.

2. Experimental

2.1. General

4-Chloro-6,7-dimethoxyquinazoline [11] **6** and 3-fluoro-5-trifluoromethylaniline [19] were prepared according to published methods. All other chemicals were purchased

from Sigma-Aldrich, Fisher Scientific or Carlo Erba. Chemicals were used as supplied, except DMSO which was passed through silica gel and stored over activated 3 Å molecular sieves for at least one day prior to use. Microwave heating was performed in a conventional oven (BR 740XL, Brother) operating at 500 W (full power). Mass spectroscopy was performed in EI mode on an LKB 2091 gas chromatograph-mass spectrometer at the Hadassah-Hebrew University mass spectroscopy facility. ^{1}H-NMR spectra were obtained on a Bruker AMX 400 MHz instrument, using tetramethylsilane as internal standard. Elemental analysis was performed at the Hebrew University microanalysis laboratory.

[18F]Fluoride ion was produced by the [18]O(p,n)[18]F nuclear reaction on ~350–600 μL enriched [18O]water (97% isotopic purity, Rotem) as a target in the Hadassah-Hebrew University IBA 18/9 cyclotron. Reactive organic [18F]fluoride ion was prepared by adding 50–100 μL irradiated target water to Kryptofix® 2.2.2 (10 mg, 27 μmol) and K_2CO_3 (1 mg, 14 μmol potassium cation) in water-acetonitrile. Azeotropic removal of water with acetonitrile was achieved by heating under a stream of nitrogen. The dried Kryptofix® 2.2.2-potassium [18F]fluoride was then dissolved in 300 μL anhydrous DMSO for use in radiolabeling.

HPLC was performed on a Varian 9012Q pump, a Varian 9050 variable wavelength detector operating at 254 nm, unless otherwise noted, and a Bioscan Flow-Count radioactivity detector with a NaI crystal. Labeled compounds were purified on a normal phase system employing a silica column (5 μm, 250 × 10 mm, Primesphere, Phenomenex (system A) or 10 μm, 500 × 9 mm, partisil, Magnum9, Whatman (system B)) and one of the following mobile phase systems (all v/v/v): system A: hexane-dichloromethane-methanol, 50:48:2; at 10 min, gradient to 35:60:5 over 30 min; 5 mL/min; or hexane-dichloromethane-2-propanol, 58:40:2; gradient to 20:70:10 over 45 min; 5 mL/min Eluent fractions (2.5 mL) were collected on a fraction collector (FC205, Gilson). Analysis of formulated radiotracers was performed on a reversed phase system using a C18 column (5 μm, 250 × 4.6 mm, Econosil, Alltech) and one of the following mobile phase systems: water-methanol, 20:80, 1 mL/min (system A); pH 4 0.1 M acetate buffer-methanol, 20:80, 1 mL/min (system B). Radiotracer formulation was performed as follows: Selected eluent fractions were transferred to a glass flask and the solution was concentrated in vacuo to dryness. To take the residue into solution one of the following two methods was used. Method A: The residue was dissolved in 0.5 mL EtOH and 0.5 mL isotonic saline. The solution was filtered through an EtOH-wetted Millex-FG filter (0.2 μm, Millipore), and another 4 mL saline was used to rinse the flask and filter, providing a 5 mL, 10% EtOH, 90% saline formulation. Method B: The residue was dissolved directly in phosphate buffered saline.

2.2. 4-[(4-Fluorophenyl)amino]-6,7-dimethoxyquinazoline (1)

Compound **6** (50 mg, 0.22 mmol) and 4-fluoroaniline (21 μL, 0.22 mmol) were placed in a dry two-neck flask and a condenser was adjusted. DMF (6 mL) was added and the mixture was heated (130°C, 30 min). After cooling, the precipitate was isolated by filtration, washed (EtOH) and dried in a vacuum oven (50°C). The product 1 was obtained as the hydrochloride salt (70 mg, 94%). ^{1}H NMR [((CD$_3$)$_2$SO) δ 9.47(s, 1H), 8.42(s, 1H), 7.8(s, 1H), 7.77(m, 2H), 7.23(m, 2H), 7.17(s, 1H), 3.94(s, 3H), 3.91(s, 3H). MS, m/e: 300 (M$^+$), 299 [(M−H)$^+$]. Anal. ($C_{16}H_{15}FClN_3O_2$): C, H, N.

2.3. 4-[(3-Fluorophenyl)amino]-6,7-dimethoxyquinazoline(4) (2)

Employing the same method used for **1**, **6** (113 mg, 0.5 mmol) and 3-fluoroaniline (48 μL, 0.5 mmol) afforded **2** as the hydrochloride salt in (166 mg, 98%). ^{1}H NMR [((CD$_3$)$_2$SO) δ 11.59(s, 1H), 8.85(s, 1H), 8.43(s, 1H), 7.7(m, 1H), 7.6(m, 1H), 7.5(m, 1H), 7.4(s, 1H), 7.1(s, 1H), 4.1(s, 3H), 3.96(s, 3H). MS, m/e: 300 (M$^+$), 299 [(M−H)$^+$]. Anal. ($C_{16}H_{15}FClN_3O_2$): C, H, N.

2.4. 4-{[3-Fluoro-5-(trifluoromethyl)phenyl]amino}-6,7-dimethoxyquinazoline (3)

Similar to **1** and **2**, **6** (113.5 mg, 0.5 mmol) and 3-fluoro-5-(trifluoromethyl)aniline [19] (93 mg, 0.52 mmol) were reacted in EtOH (8 mL) under reflux (60 min). Isolation, washing and drying yielded the hydrochloride salt of **3** (159.5 mg, 78%). ^{1}H NMR [((CD$_3$)$_2$SO) δ 8.71(s, 1H), 8.09(m, 1H), 7.64(s, 1H), 7.3(bs, 1H), 7.1(m, 1H), 7.0(m, 1H), 4.05(s, 3H), 3.90(s, 3H). MS, m/e: 368 (M$^+$). Anal. ($C_{17}H_{14}F_4ClN_3O_2$): C, H, N.

2.5. 3,4-Dichloro-6-fluoroaniline (10)

3,4-Dichloro-6-fluoronitrobenzene (**11**, 474 mg, 2.25 mmol) in 9:1 EtOH-water (7 mL) was added dropwise to a refluxing mixture of hydrazine hydrate (500 μL, 10 mmol) and Raney® nickel (60 mg, 1.4 mmol) in 7 mL EtOH-water 9:1. After the addition was completed, reflux was maintained for additional 25 min. After cooling to room temperature, the mixture was filtered and the solvent was removed in vacuo. Purification by silica gel flash column chromatography afforded **10** (193 mg, 48%). ^{1}H NMR [(CDCl$_3$) δ 7.1(d, J = 11 Hz, 1H), 6.8(d, J = 11 Hz, 1H). MS, m/e: 179 ([M−H]$^+$).

2.6. 4-[(3,4-Dichloro-6-fluorophenyl)amino]-6,7-dimethoxyquinazoline (4)

Compound **6** (128 mg, 0.56 mmol) and **10** (89 mg, 0.49 mmol) were placed in a dry two-neck flask and a condenser

was adjusted. iPrOH (6 mL) was added and the mixture heated to 85°C and treated with HCl (conc., 5 μL). Reflux was maintained for 30 min. After cooling, the precipitate was isolated by filtration, washed with EtOH and dried in a vacuum oven (50°C). Compound **4** was obtained as the hydrochloride salt (168 mg, 84%). ^{1}H NMR [(CDCl$_3$) δ 8.91(d, J = 8Hz, 1H), 8.7(s, 1H), 7.29(d, J = 10 Hz, 1H), 7.28(s, 1H), 6.9(s, 1H), 4.04(s, 3H), 4.02(s, 3H). MS, m/e: 369 (M$^+$). Anal. (C$_{16}$H$_{13}$FCl$_3$N$_3$O$_2$): C, H, N.

2.7. 4-[(3,4-Dichloro-6-fluorophenyl)amino]-6,7-dihydroxyquinazoline (5)

Compound **4** (200 mg as the HCl salt, 0.494 mmol) and pyridine hydrochloride (1.5 g, 13 mmol) were fused at 205°C for 1 h. After cooling to room temperature, water (10 mL) was added, causing a precipitate. The mixture was then placed on an ultrasonic bath for 1 h and the solid product was collected by filtration and washed with water. Recrystallization from EtOH furnished **5** as the trihydrate (35.8 mg, 18%): mp >300°C; ^{1}H NMR [(CD$_3$)$_2$SO] δ (all 1H) >12(br s), 11.1(br s), 10.5(br s), 8.71(s), 7.92(s), 7.91(d, J = 7 Hz), 7.89(d, J = 9.7 Hz), 7.42(s). MS, m/e: 305 (80%, M-Cl), 320 (98%, M-F), 322 (100%, M-OH), 339 (39%, M). Anal. (C$_{14}$H$_{14}$Cl$_2$FN$_3$O$_5$): C, H; N: calcd, 10.66; found, 10.15.

2.8. Autophosphorylation inhibition experiments in A431 cell lysate EGFr source

A431 human epidermoid (vulvar squamous cell) carcinoma cell lysate was used. A431 cells were grown in DMEM containing 10% fetal calf serum and antibiotics (penicillin and streptomycin). After several days, the cells were removed from the flasks by incubation at 37°C with PBS, 1 mM EDTA buffer for 1 hour. The pellet obtained with centrifugation of the cell suspension (600 g, 5 min, room temperature) was then resuspended in lysis buffer (0.02 M Hepes, pH 7.4, 0.125 M NaCl, 1% Triton X-100, 10% glycerol) and left on ice for 10 min. With another centrifugation (Sorval centrifuge, rotor 5, 10,000 rpm, 10 min, 4°C), the supernatant, which contained the cell lysate, was collected and frozen at −70°C in aliquots.

2.9. ELISA assay

EGFr autophosphorylation IC$_{50}$ values were obtained by means of an ELISA assay. All the following incubations were performed at room temperature and with constant shaking. After each step the plate was washed with water (5×) and TBST buffer (1×). The final volume for each well was 150 μL.

A Corning 96-well Elisa plate was coated with monoclonal anti EGFr antibody (mAb108) by incubating overnight (4°C) in a solution of mAb108 diluted in PBS (pH 8.2) [2]. After removing unbound mAb108, the plate was washed, and PBS, containing 5% milk (1% fat), was added

to block the unbound sites in the plate (25 min). An aliquot of A431 cell lysate was thawed, diluted in PBS and added to the plate.

After 25 min, seven different concentrations of each inhibitor were added, and for each series, one well was left as a zero-inhibition control (no inhibitor) and one was left as a zero EGFr kinase control (no lysate). All inhibitors were diluted in TBS-DMSO and the final concentration of DMSO was 0.5% in each well. After an additional 25 min, and without washing the plate, ATP-MnCl$_2$ solution was added to each well, the final concentration being 3 μM ATP, 5 mM MnCl$_2$. In this step the temperature was kept at 26°C and the plate was under constant shaking. Incubation with ATP-MnCl$_2$ continued for 5 min.

To stop the phosphorylation reaction, an EDTA solution (pH 8, 20 mM final concentration) was added to each well and after 1 minute the plate was washed. Polyclonal anti-phosphotyrosine serum (Sugen Inc.) was added (dilution of antibody in TBST containing 5% milk) and the wells were incubated for 45 min.

For the colorimetric detection of phosphotyrosine in EGFr, commercial TAGO anti-rabbit peroxidase conjugate antibody was added to the cells as a TBST-5% milk solution and allowed to react for 45 min. After washing, the colorimetric reaction was initiated by adding 100 μL/well ABTS-H$_2$O$_2$ in pH 4 citrate-phosphate buffer [1]. After 5–10 min, the plate was read on Dynaytec MR 5000 Elisa reader at 405 nm. Analysis of the data was performed with GraphPad Prism, version 2.01 (GraphPad Software, Inc.).

2.10. Autophosphorylation inhibition experiments in whole A431 cells

Cells (5 × 10^5) were seeded in 6-well plates (35 mm diameter, Nalge Nunc) and grown to 60–80% confluence in DMEM (high glucose) with 10% FCS, penstrep (penicillin 10^5 units/L, streptomycin 100 mg/L) (Biological Industries, Kibbutz Beit Haemek, Israel) at 37°C, 5% CO$_2$. The cells were then exposed to serum-free medium for 18 h and afterwards treated with varying concentrations of each inhibitor for 2 h. Addition of the inhibitor vehicle made the final solution 0.05% DMSO and 0.2% EtOH. Cells were activated with EGF (20 ng/ml) for 5 min and then washed with PBS. Whole-cell lysates were made by scraping the cells into the well with 0.4 mL of Leammli buffer (10% glycerol, 3% sodium dodecyl sulfate, 5% β-mercaptoethanol, 50 mM Tris pH 6.8) containing 0.001% bromophenol blue, and then boiled for 5 min. Each sample was kept at −20°C until the protein determination assay.

The amount of protein in each lysate was determined by a filter paper assay. Aliquots (3 μL) from each extract were loaded onto a strip (1 × 3 cm) of Whatman blotting paper (3 × 10 cm) and immersed into filtered dyeing solution (0.25% comassie blue, 40% MeOH, 10% acetic acid) for 20 min at room temperature with gentle shaking. Strips were then washed (3 × 15 min) with fading solution (20%

MeOH, 7% acetic acid) and then dried. Each strip was extracted with constant shaking in sodium dodecyl sulfate (3%, 500 μL, 37°C). After 1 h the eluted samples were transferred to 96-well plates and read at 595 nm in a microplate reader (ELX 800, Biotek Instruments, Inc.). A standard curve was made using BSA (1 mg/mL). A western blot assay was performed on each sample. Identical protein amounts from each lysate were loaded onto polyacrylamide gel (6% or 10%), separated by electrophoresis (Hoefer Pharmacia Biotech Inc., San Francisco, USA) and transferred to nitrocellulose (power supply: EPS 500/400, Amersham Pharmacia Biotech; nitrocellulose extra blotting membranes: Sartorius AG, Goettingen, Germany). A standard solution of high MW was loaded as reference. For visualization of molecular weight bands, the membrane was immersed in Ponceau reagent (0.05% Ponceau, 5% acetic acid) for a few minutes, and then washed thrice with TTN (10 mM Tris pH 7.4, 0.2% Tween 20, 170 mM NaCl) and once with water. The membrane was blocked overnight in TTN containing 5% milk (1% fat) (blocking TTN) and incubated for 90 min with PY20 antiphosphotyrosine antibody (Santa Cruz Biotechnology Inc., Santa Cruz, USA) diluted 1:2,000 in blocking TTN. The membrane was washed (3 × 5 min, TTN), incubated for 90 min with a horseradish peroxidase-conjugated secondary antibody (Goat anti-mouse IgG H + L, Jackson Immuno Research Laboratories, Inc., diluted 1:10,000 in blocking TTN), and finally washed again (3 × 5 min, TTN). The membranes were incubated in a luminol-based solution (1 min, 0.1 M Tris pH 8.5, 250 μM luminol, 400 μM *p*-cumaric acid, 0.033% H_2O_2) and visualized using chemiluminescent detection. Quantification of each band was performed using Adobe Photoshop 5.0 ME and NIH image 1.16/ppc programs and the IC_{50} values were calculated using a nonlinear regression fit to a variable slope sigmoidal dose-response curve (GraphPad Prism). The above assay was performed twice for each compound.

2.11. Cell growth assay

Cells (3000/well) were seeded in 96-well plates and grown for 96 h in 200 μL/well DMEM/10% FCS/penstrep. The medium was changed every 24 h for three days, adding inhibitor over a wide range of concentrations with each change.

The inhibition of growth was detected by a methylene blue assay. Plates corresponding to 0 (no inhibitor, control), 24, 48 and 72 hours were fixed by adding glutyraldehyde to each well (0.05% final concentration), incubating for 10 min at room temperature. After washing and drying, the plates were wetted with borate buffer and stained with methylene blue (100 μL/well, 1% in 0.1 M borate buffer pH 8.5, 60 min, room temperature). The plates were then washed thoroughly to remove excess dye and dried. The dye taken up by cells was extracted in 0.1 N HCl (60 min, 37°C) and the resulting solution was read (Dynatec MR500 ELISA Reader) at 620 nm. One experiment was performed for each inhibitor and 8 wells were used for each concentration.

2.12. Radiochemistry 4-[(4-[^{18}F]Fluorophenyl)amino]-6,7-dimethoxyquinazoline ([^{18}F]1)

The Kryptofix® 2.2.2-potassium [^{18}F]fluoride—DMSO solution described above was added to 1,4-dinitrobenzene (2–3 mg, 12–18 μmol) in a screw-top test tube (8 mL, Corning). The tube was capped, shaken and heated in the microwave for 3.5 min. After cooling in an ambient water bath, the vial contents were diluted with 10 mL water and loaded onto an activated (EtOH) and equilibrated (water) C18 Sep-Pak® (classic, short body, Waters). The cartridge was washed with water (10 mL) and the desired intermediate, 4-[^{18}F]fluoro-1-nitrobenzene, was eluted with EtOH (2 mL) into a small glass test tube. The reduction vessel was prepared by adding to a flat-bottomed glass vial (25 mL), sequentially, a few borosilicate glass beads, 100 μL 4:1 EtOH-water, Raney® Ni (50% slurry in water, ~250 μL) and hydrazine monohydrate (60 μL, 1.2 μmol). After capping with a septum-equipped screw cap (vented with a large diameter needle) the vial was shaken and placed in a 40°C heating block. The ethanolic 4-[^{18}F]fluoro-1-nitrobenzene solution was diluted with 0.5 mL water and added slowly to the reduction vessel. After 5 min, the vessel was cooled in an ambient water bath, and the vial contents were filtered through a 0.45 μm filter (Puradisc, polypropylene, Whatman) into another flat-bottomed 25 mL vial. To the filtered solution were added 8 mL water and 10 mL ether and by capping and inverting several times to mix, the reduction product, 4-[^{18}F]fluoroaniline, was extracted into the ether layer. An 8 mL screw-top test tube was charged with 4-chloro-6,7-dimethoxyquinazoline (4–5 mg, 17–22 μmol) and 2-propanol (300 μL). The ethereal radioaniline solution was added to the tube by passing it through $MgSO_4$ (2 g) and a new 0.45 μm filter. The ether was removed under He, warming the tube in an ambient water bath. Concentrated HCl (1 μL, 12 μmol) was added and the capped tube was heated in a 110°C oil bath for 15 min. After cooling the tube in ambient water, the acid was neutralized and the free base liberated with the addition of aqueous NaOH (5 M, 50 μL, 250 μmol). Dichloromethane (0.3 mL) and hexane (0.3 mL) were added to the tube and the solution was filtered through a 0.2 μm filter (Acrodisc, nylon, Gelman) and injected onto the normal phase HPLC (semi-preparative system A). [^{18}F]1 eluted with a t_R of 33.7 min and was formulated as described with a yield of 11% from potassium [^{18}F]fluoride. The formulation was then analyzed by reversed phase HPLC (t_R = 8.76 min; chemical purity = 89%; radiochemical purity > 95%). At formulation, [^{18}F]1 had a specific radioactivity of 363 Ci/mmol (13 GBq/μmol).

2.13. 4-[(3-[^{18}F]Fluoro-5-trifluoromethylphenyl)amino]-6,7-dimethoxyquinazoline ([3'-^{18}F]3)

The general procedure was similar to that used to synthesize [^{18}F]1 described above, with the following exceptions: In the place of 1,4-dinitrobenzene, 3,5-dinitrobenzo-

trifluoride (2–3 mg, 8–13 μmol) was used in the reaction with [^{18}F]fluoride ion to provide 3-[^{18}F]fluoro-5-nitrobenzotrifluoride; in the place of a liquid-liquid extraction following the reduction step, a second C18 Sep-Pak extraction was used, and elution of 3-[^{18}F]fluoro-5-(trifluoromethyl)aniline was achieved with ether (2 mL). HPLC purification (system A, t_R = 36.4 min) provided **[3′-^{18}F]3**. Formulated **[3′-^{18}F]3** (7% overall yield) was analyzed by reversed phase HPLC (system A, t_R = 11.6 min), indicating >95% radiochemical purity, >95% chemical purity and 460 Ci/mmol (17 GBq/μmol) specific radioactivity at formulation.

2.14. 4-[(3,4-Dichloro-6-[^{18}F]fluorophenyl)amino]-6,7-dimethoxyquinazoline ([^{18}F]4)

The general procedure was similar to that used to synthesize **[3′-^{18}F]3** described above, with the following exception: In the place of 3,5-dinitrobenzotrifluoride, 1,2-dichloro-4,5-dinitrobenzene (2–3 mg, 8–13 μmol) was used in the reaction with [^{18}F]fluoride ion to provide 1,2-dichloro-4-[^{18}F]fluoro-5-nitrobenzene. Normal phase HPLC (system B, t_R = 31.7 min) provided **[^{18}F]4**. Formulated **[^{18}F]4** (4% overall yield) was analyzed by reversed phase HPLC (system B, t_R = 9.1 min) indicating >95% radiochemical purity and ~90% chemical purity, averaging 1484 Ci/mmol (54.9 GBq/μmol) specific radioactivity.

2.15. In vitro studies with [^{18}F]4 determination of dissociation rate constant (k_{off}) and association rate constant (k_{on})

A431 cells ($1.0 \times 10^5 - 1.5 \times 10^5$) were seeded in 35 mm petri dishes (Nalge Nunc International) in 1 mL of DMEM/10% FCS/penstrep for 15–30 h. The amount of cells used for each experiment was calculated by considering the multiplication rate [6] for the A431 cell line (0.0417/hour). The dishes were kept on ice and shaken automatically throughout the radiotracer experiments.

2.16. Dissociation experiments

Each dish was incubated on ice for 30 min, then **[^{18}F]4** was added, incubating for an additional 30 min on ice. Dissociation of **[^{18}F]4** from EGFr-TK was initiated by adding unlabeled inhibitor (final concentration 10 μM inhibitor, 0.2% DMSO, 0.2% EtOH) and it was stopped by removal of medium after 1, 2, 4, 6, 10, 15, 20, 25 or 30 min, followed by two washes with cold PBS. Cells were harvested by detaching and lysing them with NaOH (0.1 M, 200 μL, 3×). Lysate and cell residue (scraped using a glass cover slip) were transferred into a counting vial. The samples, each including the glass cover slip, were counted in a γ-counter. The experiment was performed in duplicate with two to three samples used for each time point. The value k_{off} was obtained using a nonlinear regression fit to a one-phase exponential decay (GraphPad Prism).

2.17. Association experiments

Prior to addition of radiotracer, each dish was incubated on ice for 1 h. For determination of nonspecific binding, in one series, unlabeled inhibitor (final concentration 10 μM inhibitor, 0.2% DMSO, 0.2% EtOH) was added 30 min prior to tracer. **[^{18}F]4** (20 μL, 0.8 μg/mL average concentration, 1600 Ci/mmol average specific radioactivity) was then added to each dish and binding was stopped at the same time points used in the dissociation experiments. The cells were washed, harvested and counted as described above. The study was performed in duplicate and, for each replicate, four samples were used for each time point (two for total binding and two for non-specific binding). The observed association rate constant (k_{obs}) was obtained using a nonlinear regression fit to a one phase exponential association curve (GraphPad Prism) and k_{on} was calculated from k_{obs}, k_{off} and the concentration of radioligand. The equilibrium dissociation constant (K_d) was calculated by dividing the average k_{off} by the average k_{on}.

2.18. Determination of the equilibrium dissociation constant (K_d) and the maximum number of binding sites (B_{max}) in saturation studies

A431 cells (2×10^5/well) were seeded in 24-well plates (Nalge Nunc International) for 15–30 h in 1 mL medium (see above). After equilibrating the plates at room temperature (30 min), **[^{18}F]4** was added to each well over a range of concentrations (5 to 80 nM, ligand non-depletion conditions) for the determination of total binding. In paired wells, tracer was added in the same concentration as above but with unlabeled inhibitor added to a final concentration of 10 μM for the determination of nonspecific binding. Incubation continued for 30 min with shaking and at room temperature. The monolayers were then washed and counted as described above. This experiment was performed four times, each time with four samples per concentration.

2.19. In vivo biodistribution studies with [^{18}F]1 and [^{18}F]4 tumor-bearing mouse model

All experiments on living animals were performed under the guidelines and with the permission of the Research Animal Ethics Committee of The Hebrew University of Jerusalem. A nude mouse tumor implant model was developed. Balb cBy nu/nu male mice (4–10 weeks) were injected s.c. in the left or right posterior leg with A431 cells (3×10^6 in 200 μL sterile PBS). Tumor growth was checked every 2–3 days by calipers. One to two weeks after inoculation, the mice were ready to be used in ex vivo or PET studies.

2.20. In vivo biodistribution studies

Tumor bearing mice were anesthetized with pentothal (85 mg/Kg, ip) and injected iv in the tail with ^{18}F-tracer in

PBS (10–20 μCi in ~50 μL, <10% EtOH, with an average of tracer concentration ~0.121 μg/mL). Animals were sacrificed at specific time points by means of CO_2 asphyxiation. Blood and certain organs and tissues were collected or excised, counted in a γ-counter and weighed. A standard solution was prepared for the calculation of the exact amount of radioligand injected in each animal. For determination of nonspecific binding, [18F]-tracer plus nonlabeled compound were coinjected in another group of animals, and the animals were sacrificed at the same time points. The injected solution was ~10–20 μCi in ~50 μL <1% DMSO and <10% ethanol, with 10% of a 520 μM solution of **4** and 90% of [18F]-tracer, mass ratio [18F]-tracer: **4** = 1:500.

In the calculations of the binding, only those animals in which the tail injection was certainly successful were considered.

2.21. PET studies

PET scans were performed in 2D mode on the Positron Corporation HZL/R scanner (intrinsic spatial resolution: in-plane 6.4 mm at 2 mm bin size, axial 6.3 mm). The mice were anesthetized and placed supine on a flat polystyrene foam support, with feet taped to the support to minimize likelihood of movement during the scans. Transmission scans (duration 8 minutes), were obtained using a Ge-68 rotating rod. **[18F]4**, with and without unlabeled compound (as described for ex-vivo experiments), or **[18F]FDG** (~15 μCi in 50 μL of physiological solution) were then injected either into a tail vein or directly into the heart, and scan was started immediately. Dynamic emission scans were obtained starting at the time of injection, and continuing for 60 minutes (15*2 minute time frames, followed by 6*5 minute frames). PET data were normalized for variations in detector sensitivity, and corrected for wobble, randoms, scatter and deadtime. Attenuation correction was applied using the measurement transmission scan data. PET images were reconstructed both by filtered back-projection using a Butterworth filter (cut-off 0.8 cycles/mm, order 10) and by iterative reconstruction (OSEM) method. Regions of interest (ROI's) were drawn for tumor, brain and liver, and time activity curves (TAC's) were calculated for ROI's from the entire dynamic sequence of images. Each animal was then sacrificed and conventional ex vivo radiotracer biodistribution was determined as above.

2.22. Metabolite analysis in control animals

The blood metabolic profiles of the labeled inhibitors [18F]1 and [18F]4 were determined by thin layer chromatography (TLC). After injecting control mice with [18F]-tracer (tail vein), blood was collected (~0.5 mL) and divided into two portions. One portion was weighed and counted in a γ-counter for determination of %ID/g. The other portion was weighed, heparinized and extracted with ether (5 mL). The ether layer was removed, dried over magnesium sulfate

(2 g) and filtered (Whatman, Puradisc 0.5 μm, polypropylene). The ethereal solution was concentrated under a stream of helium gas to about 100 μL. Half of this concentrated solution was spotted onto the preadsorbant zone of one of each reversed phase (C18, 5 × 20 cm, 250 μm layer thickness, LKC18F, Whatman) and normal phase (silica, 60 Å, 5 × 20 cm, 250 μm layer thickness, Whatman) TLC plates. Reversed phase development was MeOH-0.1 N NaCl 4:1 and normal phase was MeOH-dichloromethane 1:9. Plates were read on a System 200 Imaging Scanner (Bioscan). The extracted blood residue was then counted in a γ-counter for determination of unextracted residual radioactivity. For [18F]4, studies were performed in kidney and liver homogenates as well, using the general procedure for the blood samples. Homogenates were formed in a tissue grinder (Fenbroek). The R_f values of the standards were (reversed phase/normal phase) as follows: 4 (0.32/0.65), 5 (0.34/0.11), 10 (0.44/0.70).

3. Results

3.1. Chemistry

Compound **1** was obtained in 94% yield as the hydrochloride salt by coupling reaction of 4-chloro-6,7-dimethoxyquinazoline (**6**) with 4-fluoroaniline (Scheme 1). Employing the same method, **2** was obtained in 98% yield. Similar to **1** and **2**, **3** was isolated in 78% yield. Compound **10**, the precursor of **4**, is not commercially available and had to be synthesized. Fluorination of 1,2-dichloro-4,5-dinitrobenzene yielded **11** in 70% yield, and **10** was obtained in 48% yield after reduction of **11** with hydrazine hydrate and Raney® nickel (Scheme 2). After coupling of **10** and **6**, compound **4** was isolated in 84% yield. Fusion reaction of **4** with pyridine hydrochloride for 1 hour furnished **5** in 18% yield (Scheme 3).

Scheme 1[a]
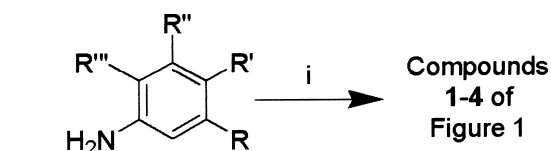
7: R, R" and R''' = H; R' = F
8: R = F; R', R" and R''' = H
9: R = F; R' and R''' = H; R" = CF₃
10: R and R' = Cl; R" = H; R''' = F

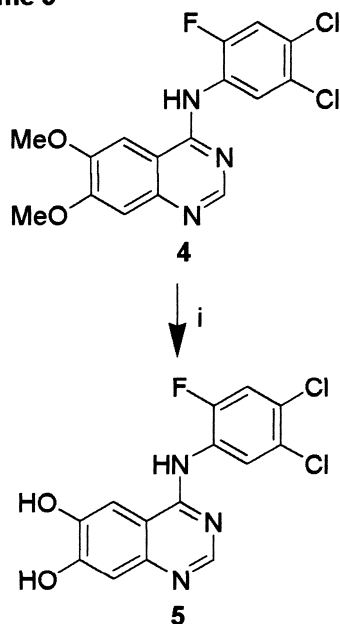[a] (i) 4-Chloro-6,7-dimethoxyquinazoline **6**/ DMF/130°C/30 min or **6**/EtOH/reflux/ 60 min or **6**/iPrOH/HCl/85°C/30 min.

Scheme 1.

Scheme 2[a]
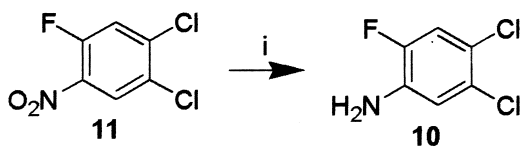
a (i) Hydrazine hydrate/Raney Ni/EtOH-H$_2$O
9:1/reflux/25 min.

Scheme 2.

Scheme 3[a]

a (i) Pyridinium hydrochloride/205°C/1 h.

Scheme 3.

3.2. In vitro screening

Two different methods were used in order to measure EGFr-TK autophosphorylation IC$_{50}$ values for the compounds and the reference inhibitors (PD 153035 and AG 1478). The first method involving cell lysate employed an ELISA assay, the second method employed intact A431 cells. The results are summarized in Table 1.

With the exception of compound **5**, which was not tested, all other compounds (**1–4**) inhibited A431 cell growth (Table 1). Compounds **4**, PD 153035 and AG 1478 were found to be potent inhibitors of cell growth with IC$_{50}$'s in the range of 1–10 μM. Compounds **1–3** were less potent inhibitors of cell growth with IC$_{50}$'s in the range of 10–20 μM.

3.3. Radiochemistry

Starting from *N,N,N*-trimethyl-3-nitroanilinium iodide, ^{18}F radiolabeling of **2** was achieved in very low yield

(~1%). Compounds **1**, **3** and **4** were prepared according to Scheme 4, following the same synthetic strategy used to make the nonlabeled compounds. A symmetrical aryl dinitro derivative **12**, **13** or **14** was reacted with organic [^{18}F]fluoride ion in DMSO, using a conventional microwave oven to heat the reaction mixture, to give the corresponding aryl [^{18}F]fluoronitro derivative in estimated yields of 60–80%. The remaining single nitro residue was reduced to an amino residue with Raney® nickel at 40°C. From the [^{18}F]fluoronitros [^{18}F]15, [3'-^{18}F]16 and [^{18}F]11, [^{18}F]fluoroaniline yields averaged ~75%. After ether evaporation and acidifying the reaction mixture, the reactions proceeded to the final labeled tracers, [^{18}F]1, [3'-^{18}F]3 and [^{18}F]4, in overall non-decay-corrected yields of 4–12% (from potassium [^{18}F]fluoride kryptand). The entire process was completed within ~120–150 min of radionuclide production. In all cases, the products were radiochemically pure.
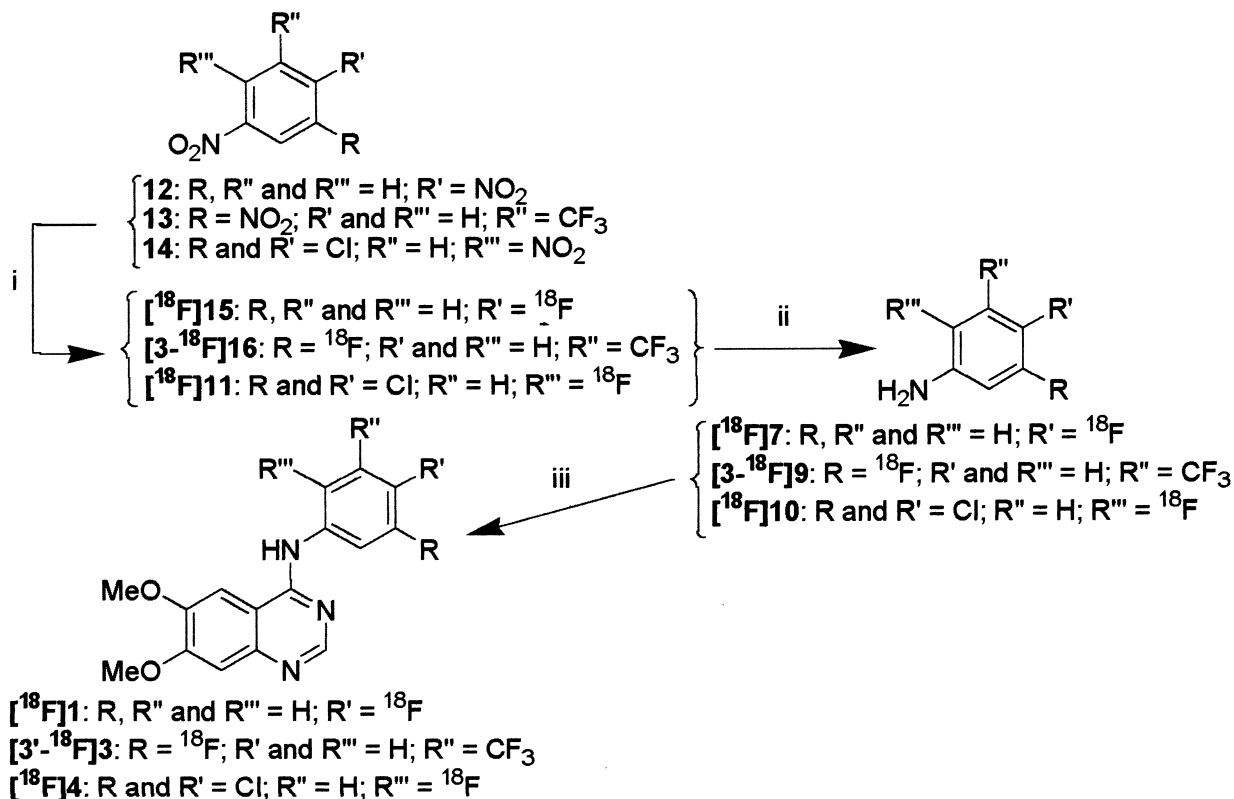
3.4. Radiotracer in vitro studies

Our labeled lead, [^{18}F]4, was studied in vitro to determine its equilibrium dissociation constant (K$_d$) and its ability to measure B$_{max}$ in receptor saturation experiments in A431 cells. In this study, a K$_d$ of 21 $\pm$ 14 nM was obtained and an average B$_{max}$ of 1.18×10^6 ($\pm 0.77 \times 10^6$) binding sites per cell was measured. In a binding kinetic study association and dissociation rates (k$_{on}$, k$_{off}$) constants of 2.57×10^6 ($\pm 1.61 \times 10^6$) M^{-1} min^{-1} and 0.169 (± 0.038) min^{-1} respectively were measured. The K$_d$ value derived from these kinetic studies was 65 nM.

3.5. Radiotracer in vivo studies

In vivo biodistribution experiments performed in tumorbearing nude mice with the two most potent labeled compounds, [^{18}F]1 and [^{18}F]4, demonstrated neither high nor specific binding in the EGFr-TK-rich tumor. With [^{18}F]1, which was studied at 30 and 60 minutes, we observed tumor uptake at levels of 1.14 and 1.34 %id/g, respectively (Table 2).

Experiments with high affinity [^{18}F]4 (Table 3), which was studied at 5, 10 and 30 minutes indicated high levels of radioactivity in the kidneys and liver in all cases. Uptake of [^{18}F]4 was observed in the tumors at a level somewhat higher than with [^{18}F]1. Blocking was suggested only at the 10 minutes time point, although the error in the non-blocked experiment was large. Tumor to blood ratios were below unity in all cases.

PET scanning for the mice was carried out on a regular whole body PET scanner. Tumor bearing mice were injected either with [^{18}F]FDG or with [^{18}F]4. Fig. 2 shows the time/activity curves of the two tracers in the tumors, and Fig. 3 presents the comparison between images obtained in the time frames of highest tumor uptake (45–50 min for [^{18}F]FDG and 8–12 min for [^{18}F]4). The chosen images demonstrate the possibility of obtaining a fairly good reso-

Scheme 4[a]

$[^{18}F]$**1**: R, R" and R''' = H; R' = ^{18}F
$[3'-^{18}F]$**3**: R = ^{18}F; R' and R''' = H; R" = CF_3
$[^{18}F]$**4**: R and R' = Cl; R" = H; R''' = ^{18}F

[a] (i) Kryptofix K$[^{18}F]$F/DMSO/microwave heating/3.5 min; (ii) Hydrazine hydrate/Raney Ni/EtOH-H_2O 4:1/40°C/5 min; (iii) 4-Chloro-6,7-dimethoxyquinazoline 6/iPrOH/HCl/110°C/15 min.

Scheme 4.

lution for the tumor region. The ex vivo biodistribution that followed the $[^{18}F]$**FDG** PET study showed that the ratios tumor/blood and tumor/muscle were 7.76 and 6.44, respectively, at the sacrifice time (65 min).

The blood metabolic analysis of $[^{18}F]$**1** and $[^{18}F]$**4** in control mice are summarized in Table 4, and 5 respectively. At 20 minutes post injection, only 0.24 %id/g $[^{18}F]$**1** was non-metabolized and by 60 minutes, the amount decreased

Table 1
EGFr kinase and A431 cell growth inhibition by 4-(anilino)quinazolines

Inhibitor	Lysate IC$_{50}$ for EGFr-TK autophosphorylation* (nM)		Whole cell IC$_{50}$ for EGFr-TK autophosphorylation[†‡‡] (nM)		IC$_{50}$ ratio: whole cell to lysate	Approximate IC$_{50}$ for cell growth (μM)
1	75.4[‡]	(34.1–167)	3230	(1350–5100)	43	10
2	17.4[§]	(10.8–28.0)	1180	(700–1650)	68	10–20
3	199[§]	(73–542)	970	(500–1440)	5	≥12.5
4	0.208[§]	(0.032–1.37)	3.8	(2.9–4.7)	18	4.5
5	1117**	[680]	[††]	—	—	[††]
PD153035	0.187[‡‡]	(0.069–0.511)	14.6	(13.3–15.9)	77	2.9
AG1478	0.719[‡]	(0.304–1.70)	3.55	(2.6–4.5)	5	1–10

* Ninety-five percent confidence interval shown in parentheses or SD shown in square brackets.
[†] Range shown in parentheses.
[‡] N = 4.
[§] N = 3.
** Individual curves were fit and IC$_{50}$ values were averaged to give this value; N = 5.
[††] Not determined due to the high IC$_{50}$ value found in cell lysate.
[‡‡] N = 2.

Table 2
Biodistribution of [^{18}F]1 in tumor-bearing mice

Tissue	%id/g*			
	30 min†		60 min‡	
Blood	1.89	[1.64/2.14]	0.79	[0.15]
Brain	0.21	[0.13/0.29]	0.14	[0.05]
Heart	1.94	[1.47/2.41]	0.81	[0.32]
Kidney	3.59	[2.69/4.48]	1.47	[0.64]
Liver	2.3	[1.68/2.92]	0.97	[0.16]
Lung	2.24	[1.95/2.53]	0.9	[0.33]
Skin	1.56	[1.35/1.78]	§	—
Spleen	1.19	[0.90/1.48]	0.51	[0.21]
Testes	0.66	[0.51/0.81]	0.41	[0.18]
Tumor	1.14	[0.89/1.39]	1.34	[0.79]

Tissue	Tissue/blood			
	30 min		60 min	
Brain	0.11	[0.08/0.14]	0.18	[0.03]
Heart	1.01	[0.89/1.13]	1.01	[0.26]
Kidney	1.87	[1.64/2.10]	1.82	[0.52]
Liver	1.2	[1.02/1.37]	1.23	[0.14]
Lung	1.19	[1.18/1.19]	1.12	[0.26]
Skin	0.83	[0.82/0.83]	§	—
Spleen	0.62	[0.55/0.69]	0.63	[0.16]
Testes	0.34	[0.31/0.38]	0.52	[0.27]
Tumor	0.6	[0.54/0.65]	1.62	[0.68]

* Percent injected dose of radiotracer per gram of wet tissue. Means are given with SD for n = 3, or the range of the two values for n = 2 (square brackets).
† N = 2.
‡ N = 3.
§ Not taken.

8-fold; at 10 minutes post injection, 0.60 %id/g [^{18}F]4 was non-metabolized. In the case of [^{18}F]4, since we studied the blood, kidney and liver all at 10 minutes both in tumor-bearing mouse biodistribution experiments and in metabolic analysis, we can describe the amount of radiotracer left unaltered in relation to the total radioactivity found in the respective tissue. Assuming the distribution of the tracer is similar in both models, only 14% of blood radioactivity, 14% of kidney radioactivity and 10% of liver radioactivity found in the biodistribution experiments is intact [^{18}F]4.

4. Discussion

In our search for ^{18}F-labeled EGFr-TK PET tracers, we prepared compounds **1–5**, each related structurally to the potent inhibitors PD153035 and AG1478, as candidates for future ^{18}F-labeling (Fig. 1). We chose the aniline ring for structural modification to suit our radiolabeling strategy, and, in addition to fluorine, we selected the electron withdrawing groups CF$_3$ and Cl for substitution on the ring. To identify the lead compounds for PET imaging, and to evaluate their potential for use as drugs, we performed a series of in vitro studies. EGFr autophosphorylation inhibition was

measured in A431 cell lysate and intact cells, and cell growth inhibition was measured in the same cell line. Labeling chemistry was then developed for three of the compounds, leading to in vitro evaluation of the lead tracer, ex vivo biodistribution studies with two tracers, and in vivo PET studies with the lead tracer.

4.1. Chemistry

Compounds **1–4** were prepared by coupling 4-chloro-6,7-dimethoxyquinazoline **6** with the corresponding aniline derivatives **7–10** in dimethylformamide (DMF), ethanol (EtOH) or acidic 2-propanol (iPrOH) (Scheme 1). Two of the anilines are not commercially available and had to be synthesized. Compound **9** was made as described [19] and **10** was made in a similar fashion (see Scheme 2).

Based on a report of similar compounds, removal of one or both methyl groups from a potent 4-anilino-6,7-dimethoxyquinazoline results in a compound only moderately less potent than the parent [23]. Thinking that we could maintain some of the potency of **4**, while decreasing considerably its lipophilicity, we cleaved the methyl groups on **4** to provide **5** (Scheme 2). Since the 6- and 7-des-methyl derivatives have been reported to be two of four observed metabolic products of PD153035, [14] we also hoped that **5** would have been a metabolically stable alternative to **4**.

4.2. Screening for EGFr-TK inhibition potency

Using two different methods, EGFr-TK autophosphorylation IC$_{50}$ values were measured for the compounds and the reference inhibitors (PD153035 and AG1478) to determine their potential as PET tracers. The results are summarized in Table 1.

The first method, involving cell lysate and thus not requiring that the compounds cross a cell membrane, employed an ELISA assay. For **1**, substitution of a fluorine atom at the para position on the aniline ring resulted in a moderate IC$_{50}$ of 75.4 nM compared to PD153035 (IC$_{50}$ = 0.187 nM) and AG1478 (IC$_{50}$ = 0.719 nM). In the case of **2**, [4] a fluorine atom at the meta position increased the biological activity about 4-fold compared to **1**. Compound **2** was still, however, less potent (IC$_{50}$ = 17.4 nM) than the reference inhibitors, each having a heavier halogen at the meta position of the aniline ring. Compound **3**, containing the trifluoromethyl group at the 5′ position in addition to the fluorine atom at the meta position, was less potent (IC$_{50}$ = 199 nM) than either **1** or **2**. Based on the IC$_{50}$ values for the EGFr-TK autophosphorylation in A431 lysate, **4** was found to be the most potent inhibitor of the four fluorinated dimethoxy compounds with an IC$_{50}$ of 0.21 nM, reflecting the importance of the chlorine atom (i.e. a heavier halogen, see above) at the meta position. The addition of a chlorine atom at the para position and fluorine at the 6′ position contributed to the potency of **4**, resulting in an IC$_{50}$ value lower than that of AG1478. Unfortunately, after methyl group cleavage, a near complete loss of potency was observed for **5** (IC$_{50}$ = 1117 nM).

Table 3
Biodistribution of [^{18}F]4 in tumor-bearing mice

tissue	%id/g*									
	5 min[†]		10 min[‡]		10 min blocked[§]		30 min**		30 min blocked[††]	
Bladder	1.28[‡‡]	—	1.61	[0.84]	1.98	[1.41/2.56]	19.55	[15.89]	40.40	[1.90/78.90]
Blood	3.44	[0.89]	4.34	[1.66]	3.22	[2.45/3.99]	4.83	[1.36]	5.88	[4.08/7.69]
Brain	4.37	[1.01]	4.05	[0.68]	4.36	[3.25/5.48]	2.02	[0.38]	2.75	[1.65/3.84]
Heart	6.51	[1.77]	5.95	[1.12]	6.73	[5.40/8.06]	4.25	[0.22]	5.01	[3.35/6.67]
Kidney	11.20	[2.77]	14.81	[5.47]	10.95	[8.43/13.48]	20.49	[7.64]	22.68	[10.34/35.03]
Liver	14.87	[3.15]	17.60	[4.48]	15.18	[17.71/12.66]	15.30	[1.50]	17.84	[14.10/21.58]
Lung	5.44	[1.01]	5.49	[1.59]	5.80	[4.29/7.31]	4.94	[0.63]	5.59	[4.01/7.17]
Muscle	4.40	[2.50]	3.41	[1.81]	2.65	[2.54/2.76]	2.35	[1.02]	3.83	[3.61/4.05]
Skin	4.37	[2.05]	4.37	[1.61]	3.10	[2.75/3.44]	3.57	[0.62]	7.50	[6.14/8.85]
Testes	3.07	[0.60]	3.54	[1.02]	2.71	[2.48/2.94]	2.34	[0.42]	3.97	[2.04/5.91]
Tumor	2.90	[1.67]	2.83	[3.07]	0.91	[0.68/1.14]	1.95	[0.80]	3.47	[3.29/3.65]
					Tissue/blood					
Tissue	5 min		10 min		10 min blocked		30 min		30 min blocked	
Bladder	0.29	—	0.32	[0.21]	0.49	[0.35/0.64]	5.44	[5.45]	9.79	[0.25/19.33]
Brain	1.28	[0.09]	1.03	[0.38]	1.08	[0.80/1.37]	0.46	[0.24]	0.45	[0.41/0.50]
Heart	1.91	[0.32]	1.48	[0.45]	1.67	[1.32/2.02]	0.95	[0.36]	0.84	[0.82/0.87]
Kidney	3.28	[0.39]	3.45	[0.66]	2.72	[2.07/3.38]	4.16	[0.46]	3.54	[2.53/4.56]
Liver	4.45	[1.14]	4.28	[0.98]	3.77	[3.10/4.44]	3.30	[0.71]	3.13	[2.81/3.45]
Lung	1.62	[0.30]	1.32	[0.26]	1.44	[1.05/1.83]	1.06	[0.19]	0.96	[0.93/0.98]
Muscle	1.31	[0.78]	0.77	[0.21]	0.66	[0.62/0.69]	0.47	[0.09]	0.71	[0.53/0.88]
Skin	1.25	[0.37]	1.04	[0.31]	0.77	[0.67/0.86]	0.76	[0.11]	1.33	[1.15/1.51]
Testes	0.90	[0.11]	0.91	[0.45]	0.67	[0.61/0.74]	0.50	[0.07]	0.63	[0.50/0.77]
Tumor	0.89	[0.63]	0.55	[0.37]	0.23	[0.17/0.29]	0.39	[0.06]	0.64	[0.47/0.81]

* Percent injected dose of radiotracer per gram of wet tissue. Means are given with SD for n ≥ 3 and the range of the 2 values for n = 2 (square brackets).
[†] n = 3.
[‡] n = 5.
[§] n = 2.
** n = 3.
[††] n = 2.
[‡‡] n = 1.

The second method of measuring each compound's potency to inhibit EGFr-TK autophosphorylation employed intact A431 cells thus requiring that the compounds cross a cell membrane. Evaluation of **5** in whole cells was not warranted since it was shown to be a very weak inhibitor in lysate. Compounds **1–4** were 5- to 68-fold less potent in
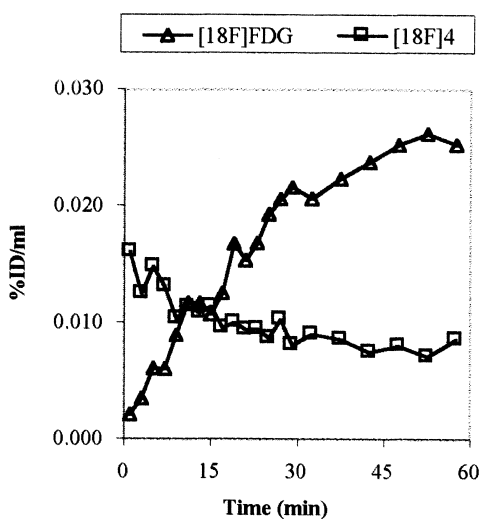

Fig. 2. Activity concentration in tumor of tumor bearing mice injected with [^{18}F]FDG by the heart and [^{18}F]4 by the tail vein.
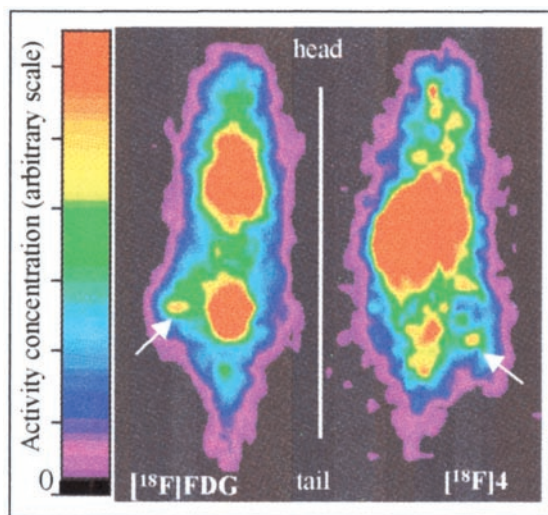

Fig. 3. PET images (coronal slices) of mice: Left: 45–50 minutes post [^{18}F]FDG heart injection, tumor in the right leg. Right: 8–12 minutes post [^{18}F]4 tail injection, tumor in the left leg. Arrows indicate the tumor areas.

Table 4
Results of [^{18}F]1 blood metabolite analysis in control mice. Means are given with SD for n = 3 and with the range of the two values for n = 2 (in square brackets).
A. 1-(post-extraction blood counts/pre-extraction blood counts).
B. Value in column A multiplied by blood %id/g at the specified time.
C. Average of reverse and normal phase TLC results.
D. Value in column B multiplied by value in column C.

Time (min)	A Extracted fraction of blood radioactivity		B Extracted fraction normalized to %id/g		C Non-metabolized fraction of [^{18}F]1 from TLC		D Extracted non-metabolized [^{18}F]1 normalized to %id/g	
20*	0.16	[0.02]	0.31	[0.03]	0.75	[0.13]	0.24	[0.02]
40†	0.18	—	0.21	—	0.92	—	0.19	—
60‡	0.09	[0.08/0.1]	0.05	[0.03/0.07]	0.57	[0.50/063]	0.03	[0.02/0.04]

* n = 3.
† n = 1.
‡ n = 2.

intact cells than they were in cell lysate (Table 1) and a similar trend was seen with the reference compounds. In intact cells, compound **4** remained the most potent of the dimethoxy fluorinated derivatives, with an IC$_{50}$ on par with the most potent reference compound, AG1478.

4.3. A431 cell growth inhibition

With the exception of compound **5**, which was not tested, all other compounds (**1–4**) inhibited A431 cell growth. Considering all compounds tested, a less potent inhibitor of intact cell EGFr-TK autophosphorylation (**1–3**, 970–3230 nM IC$_{50}$) was also a less potent inhibitor of cell growth (10–20 μM IC$_{50}$). In accordance, more potent inhibitors of EGFr-TK autophosphorylation in intact cells (**4**, PD153035 and AG1478; 3.55–14.6 nM IC$_{50}$) were also more potent inhibitors of cell growth (1–10 μM IC$_{50}$). Whereas the inhibition of EGFr-TK autophosphorylation clearly measures a specific effect of inhibitor on the receptor, we cannot assume that each compound inhibited cell growth exclusively through EGFr-TK inhibition, despite its high expression on A431 cells. By inference, however, we can assume that 4 inhibits growth by acting only on EGFr-TK since radiotracer binding exper-

iments indicated that **[^{18}F]4** bound with high affinity to a single site in A431 cells with the number of binding sites in the range of published values (see Radiotracer in vitro studies in this section).

4.4. Radiochemistry

Starting from N,N,N-trimethyl-3-nitroanilinium iodide, following the general strategy outlined in Scheme 3, ^{18}F radiolabeling of **2** was achieved in very low yield (~1%). The main problem in the synthesis was the first step, which provided only 10–30% of the desired 3-[^{18}F]fluoronitrobenzene. Thus work with this compound will not be discussed further as we are exploring alternate approaches to radiolabeling it.

The radiolabeling of **1**, **3** and **4** proved more successful: each compound could be prepared in a yield suitable to allow future use in biological experiments. In the reduction of the nitro groups to amino derivatives, moderate temperature and short reaction time were critical, as higher temperatures and longer times resulted in apparent over reduction of the [^{18}F]fluoroaniline and loss of radioactivity on the Raney® nickel. Before continuing with the coupling reaction, ether had to be removed from the reaction mixture.

Table 5
Results of [^{18}F]4 blood, kidney and liver metabolite analysis in control. Mice at 10 min post-injection (n = 3). Means are given with SD in square brackets.

Tissue	A Extracted fraction of blood radioactivity		B Extracted fraction normalized to %id/g		C Non-metabolized fraction of [^{18}F]4 from TLC		D Extracted non-metabolized [^{18}F]4 normalized to %id/g	
Blood	0.36	[0.04]	1.08	[0.32]	0.56	[0.11]	0.60	[0.16]
Kidney	0.39	[0.13]	3.27	[1.19]	0.67	[0.11]	2.14	[0.47]
Liver	0.27	[0.14]	2.58	[1.40]	0.68	[0.26]	1.82	[1.28]

A. 1-(post-extraction blood counts/pre-extraction blood counts)
B. Value in column A multiplied by blood %id/g at the specified time.
C. Average of reverse and normal phase TLC results.
D. Value in column B multiplied by value in column C.

Performing the ether evaporation in the presence of iPrOH was critical, as evaporation of the ether-radioaniline solution alone either in vacuo (using a rotary evaporator) or under helium gas, either with or without heating, resulted in significant or complete co-volatilization of the radioaniline.

4.5. Radiotracer in vitro studies

Study of a radiotracer's binding properties in vitro can indicate whether the tracer has potential in PET. Generally, receptor- and enzyme-binding radiotracers should bind to a single site with high affinity. Additionally, the in vivo binding potential (bound radiotracer to free radiotracer, or theoretically maximal target-to-nontarget ratio) of a radiotracer can be calculated from the concentration of target receptors in a tumor and the compound's binding affinity [8]. Our labeled lead, $[^{18}F]4$, was studied in vitro to determine its equilibrium dissociation constant (K_d) and its ability to measure B_{max} in receptor saturation experiments in A431 cells. A reliable in vitro method for the measurement of the maximum number of binding sites (B_{max}) could conceivably be used clinically to determine the EGFr concentration in tumor biopsies, allowing differential diagnosis without a PET procedure. The K_d found in the saturation experiments, 21 ± 14 nM, while approximately 5.5 times higher than the compound's whole cell IC_{50} values, indicated a high affinity radioligand for EGFr-TK. The saturation curves also indicated an average B_{max} of 1.18×10^6 ($\pm 0.77 \times 10^6$) binding sites per cell, in accord with published values for this cell line [12,13]. The experiments suggested that the tracer binds to a single site, indicating that the tracer is selective for EGFr-TK. By using a reported cell density of 1.2×10^7 A431 cells/mL of experimental A431-derived tumor [3], we calculated the binding potential of $[^{18}F]4$ as follows:

$$\text{Binding Potential (BP)} = \frac{B_{max}}{K_d}$$

$$\text{BP} = \frac{1.18 \times 10^6 \text{ EGFr molecules}}{\text{A431 cell}} \times \frac{\text{L tumor}}{21 \text{ nmol}}$$

$$\times \frac{10^9 \text{ nmol}}{6.022 \times 10^{23} \text{ EGFr molecules}}$$

$$\times \frac{1.2 \times 10^7 \text{ A431 cells}}{10^{-3} \text{ L tumor}}$$

$$\text{BP} = 1.1$$

The value of 1.1 obtained from the above calculation reveals a low ratio, meaning that $[^{18}F]4$ might not be a suitable tracer for PET. In general, a lower K_d and higher B_{max} resulting in a ratio ≥ 10 is considered a reasonable value for achieving a high target-to-nontarget ratio, hence successful imaging in vivo [8].

Specific binding site association and dissociation rates (k_{on} and k_{off}) were measured for $[^{18}F]4$ in kinetics experiments, which lead to an independent determination of K_d. Binding kinetics demonstrated an association rate constant (k_{on}) of 2.57×10^6 ($\pm 1.61 \times 10^6$) M^{-1} min^{-1} and a dissociation rate constant (k_{off}) of 0.169 (± 0.038) min^{-1}. The K_d value derived from these kinetic studies, 65 nM, was somewhat higher than the value found in the saturation experiments ($K_d = 21 \pm 14$ nM).

4.6. Radiotracer in vivo studies

In vivo biodistribution experiments performed in tumor-bearing nude mice with the two most potent labeled compounds, $[^{18}F]1$ and $[^{18}F]4$, demonstrated neither high nor specific binding in the EGFr-TK-rich tumor. With $[^{18}F]1$, which was studied at 30 and 60 min, we observed tumor uptake at levels of 1.14 and 1.34 %id/g, respectively (Table 2). Tumor to blood ratios, which should suggest specificity for EGFr-TK and potential for in vivo imaging, were below unity at 30 min and increased to only 1.62 at 60 min. Experiments with high affinity $[^{18}F]4$ (Table 3), which was studied at 5, 10 and 30 min indicated high levels of radioactivity in the kidneys and liver in all cases. Since the amount of radioactivity in these EGFr-TK-expressing organs was not decreased in the blocking studies (at 10 and 30 min), it was presumed to be due to rapid metabolism and pre-excretion processing of the tracer and not specific binding to the target receptor-kinase. Uptake of $[^{18}F]4$ was observed in the tumors at a level somewhat higher than with $[^{18}F]1$. Blocking was suggested only at the 10 min time point, although the error in the non-blocked experiment was large. Tumor to blood ratios were below unity in all cases. The high standard deviation shown in the experiments hindered any solid conclusions about tracer specificity in vivo. The large error was probably due to the different aspect of the tumors. When each animal was sacrificed the general morphological conditions were checked and nothing abnormal was noticed in all tissues, but the tumor itself was certainly different from one animal to another, in the consistency, growth and vascularization. However we could not assess the histological aspect and the vascularization level of each tumor, limiting our analysis to the measurement of volume and weight.

PET scanning for the mice was carried out on a regular whole body PET scanner with an in-plane resolution of 6.3 mm and axial resolution of 6.4 mm. In view of the small size of the mice, the purpose of the PET scans was not to map the biodistribution of the tracer, which would only have been possible with a scanner with finer resolution, but rather to provide an in vivo reality check for the ex-vivo biodistribution studies. The relatively poor resolution of the PET scanner would lead to underestimates of activity in any small focal area due to the partial volume effect. PET studies with $[^{18}F]4$ were as discouraging as the ex-vivo results. In order to verify that the low resolution of the PET camera did not contribute to the weak tumor images in the animals injected with $[^{18}F]4$, a tumor bearing mouse was

Scheme 5
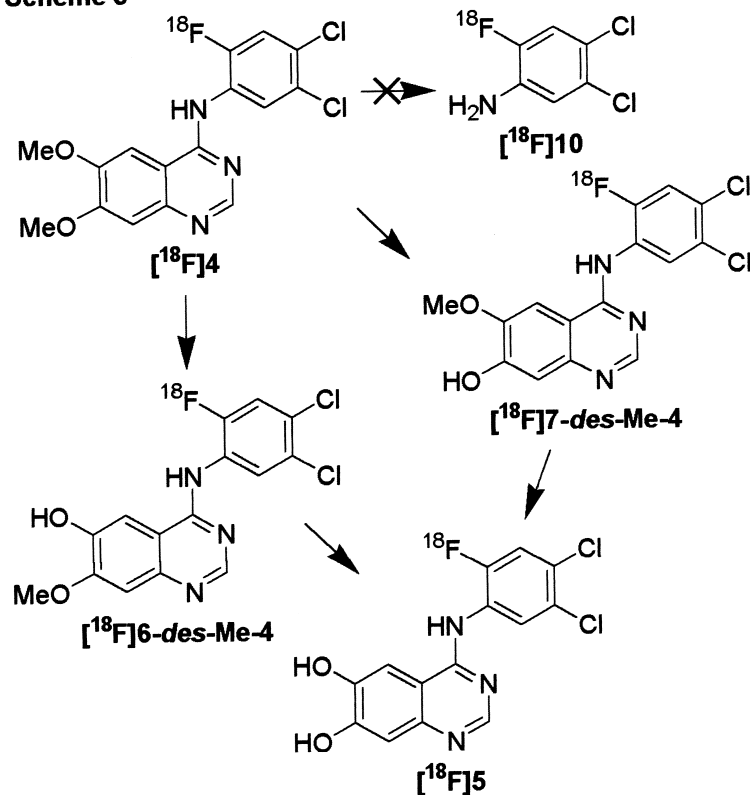
Scheme 5.

injected with [¹⁸F]FDG. In the [¹⁸F]FDG injected mouse the tumor is consistently visible and defined in every frame from 24 to 60 min, while for the animal injected with [¹⁸F]4, no one area of consistently enhanced is observed on the tumor bearing leg, except briefly from 8–12 min (Fig. 3). The [¹⁸F]FDG uptake curve (Fig. 2) clearly demonstrates the accumulation of the tracer in the tumor, while the corresponding curve for [¹⁸F]4 confirms the rapid washout of the compound from the tumor region. Note that since no blocking compound was administered, the [¹⁸F]4 uptake, as demonstrated in the images and time-activity curves, includes activity concentration due to both specific and non-specific binding during the scan. The mice were permitted to continue eating until shortly before the scans; it is possible that in the fasted state, the quality of the [¹⁸F]FDG images would have been better, with a more favorable ratio of uptake in tumor to other structures and clearer visualization of the tumor, as a result of less competition with unlabeled plasma glucose, and lower plasma insulin levels.

The ex vivo biodistribution that followed the [¹⁸F]FDG PET study showed that the ratios tumor/blood and tumor/muscle were 7.76 and 6.44, respectively, at the sacrifice time (65 min). Ratios of [¹⁸F]4 biodistribution at 10 min were 0.55 tumor/blood and 0.83 tumor/muscle. These low values support the high non-specific binding of [¹⁸F]4 observed in the PET images.

Through studies of the blood metabolic analysis of

[¹⁸F]1 and [¹⁸F]4 in control mice (Tables 4 and 5, respectively), we were able to surmise that one reason for the compounds' poor performance in vivo could be rapid degradation. We assume that only the non-metabolized tracer is available for tumor cell uptake and receptor-kinase binding. In regard to the identity of the metabolites observed, we had only one standard for [¹⁸F]1, the aniline 9. The labeled equivalent, [¹⁸F]9, was clearly not a blood metabolite at any time point studied for [¹⁸F]1. Interestingly, [¹⁸F]5 was found as a metabolite of [¹⁸F]4 in both the liver and the kidney extracts, but not the blood. The reported PD153035 metabolite study indicated the presence of both 6- and 7-*des*-methyl analogs, but not the 6,7-di-*des*-methyl analog, in blood [14]. We assume that, for [¹⁸F]4, the 6- and 7-*des*-methyl analogs are both intermediates in its transformation to [¹⁸F]5 (see Scheme 5). The radioaniline [¹⁸F]10, was not a metabolite in any of the samples analyzed with [¹⁸F]4.

5. Conclusion

In this study we show that high affinity ¹⁸F labeled reversible inhibitors of EGFr-TK might not be a suitable imaging agents. While some in vitro experiments may indicate efficacy of 4-(anilino)quinazoline compounds such as those described in this report, kinetic factors such as k_{on} and

k_{off} and rapid blood clearance apparently make them ineffective as tracers for nuclear medicine imaging of EGFr-TK. Whether the discrepancy between encouraging in vitro results and discouraging in vivo results can be explained by ATP competition at the compounds' binding site or by an intrinsic phenomenon of compound interaction at the binding site remains to be revealed.

Our study shows that in order to achieve better imaging results one would have to eliminate the non-specific ^{18}F distribution. Labeled derivatives of the recently reported irreversible inhibitors [24,25] may prove more promising as diagnostic radiotracers.

Acknowledgments

References

[1] 7.5 mg ABTS, 2 μL 30% H_2O_2, 15 mL pH 4 citrate-phosphate buffer

[2] Since the exact concentrations of mAb108 in the stock solution and EGFr in the cell lysate were unknown, an autophosphorylation experiment was performed to determine the optimal dilution of mAb108 stock and lysate. Stock mAb108 (approx. 0.2–0.5 mg/mL) was diluted 1:400, 1:600, 1:800 and 1:1000 with PBS, while A431 cell lysate was diluted 1:2, 1:4, 1:6, 1:8, and 1:10. After obtaining results from every possible mAb108-lysate dilution combination, the chosen dilutions of mAb108 and A431 cell lysate were those which gave optical densities around 1.2–1.4 with added ATP and 0.09–0.1 for the control group (without ATP).

[3] M.J. Allalunis-Turner, D.W. Siemann, Recovery of cell subpopulations from human tumour xenografts following dissociation with different enzymes, *Br. J. Cancer* 54 (4) (1986) 615–622.

[4] A.J. Bridges, H. Zhou, D.R. Cody, G.W. Rewcastle, A. McMichael, H.D. Showalter, D.W. Fry, A.J. Kraker, W.A. Denny, Tyrosine kinase inhibitors, 8, An unusually steep structure-activity relationship for analogues of 4-(3-bromoanilino)-6,7-dimethoxyquinazoline (PD153035), a potent inhibitor of the epidermal growth factor receptor, *J. Med. Chem.* 39 (1) (1996) 267–276.

[5] J. Capala, R.F. Barth, M.Q. Bailey, R.A. Fenstermaker, M.J. Marek, B.A. Rhodes, Radiolabeling of epidermal growth factor with ^{99m}Tc and in vivo localization following intracerebral injection into normal and glioma-bearing rats, *Bioconjug. Chem.* 8 (3) (1997) 289–295.

[6] J.M. Davis, Basic Cell Culture—A Practical Approach, IRC Press, Oxford.

[7] C.R. Divgi, S. Welt, M. Kris, F.X. Real, S.D. Yeh, R. Gralla, B. Merchant, S. Schweighart, M. Unger, S.M. Larson et al., Phase I and imaging trial of indium 111-labeled anti-epidermal growth factor receptor monoclonal antibody 225 in patients with squamous cell lung carcinoma, *J. Natl. Cancer Inst.* 83 (2) (1991) 97–104.

[8] W.C. Eckelman, Sensitivity of new radiopharmaceuticals, *Nucl. Med. Biol.* 25 (3) (1998) 169–173.

[9] A. Fredriksson, P. Johnstrγm, J.O. Thorell, G. von Heijne, M. Hassan, S. Eksborg, P. Kogner, P. Borgstrγm, M. Ingvar, S. Stone-

[10] D.W. Fry, A.J. Kraker, A. McMichael, L.A. Ambroso, J.M. Nelson, W.R. Leopold, R.W. Connors, A.J. Bridges, A specific inhibitor of the epidermal growth factor receptor tyrosine kinase, *Science* 265 (5175) (1994) 1093–1095.

[11] A. Gazit, J. Chen, H. App, G. McMahon, P. Hirth, I. Chen, A. Levitzki, Tyrphostins IV—highly potent inhibitors of EGF receptor kinase, Structure-activity relationship study of 4-anilidoquinazolines, *Bioorganic And Medicinal Chemistry* 4 (8) (1996) 1203–1207.

[12] A. Goldenberg, H. Masui, C. Divgi, H. Kamrath, K. Pentlow, J. Mendelsohn, Imaging of human tumor xenografts with an indium-111-labeled anti-epidermal growth factor receptor monoclonal antibody, *J. Natl. Cancer Inst.* 81 (21) (1989) 1616–1625.

[13] H. Haigler, J.F. Ash, S.J. Singer, S. Cohen, Visualization by fluorescence of the binding and internalization of epidermal growth factor in human carcinoma cells A-431, *Proc. Natl. Acad. Sci. USA* 75 (7) (1978) 3317–3321.

[14] M.W. Kunkel, K.E. Hook, C.T. Howard, S. Przybranowski, B.J. Roberts, W.L. Elliott, W.R. Leopold, Inhibition of the epidermal growth factor receptor tyrosine kinase by PD153035 in human A431 tumors in athymic nude mice, *Investigational New Drugs* 13 (4) (1996) 295–302.

[15] A. Kurihara, Y. Deguchi, W.M. Pardridge, Epidermal growth factor radiopharmaceuticals: ^{111}In chelation, conjugation to a blood-brain barrier delivery vector via a biotin-polyethylene linker, pharmacokinetics, and in vivo imaging of experimental brain tumors, *Bioconjug. Chem.* 10 (3) (1999) 502–511.

[16] A. Levitzki, A. Gazit, Tyrosine kinase inhibition: an approach to drug development, *Science* 267 (5205) (1995) 1782–1788.

[17] J.K. Lim, D.J. Riese, K. Negash, R.A. Hawkins, H.F. VanBrocklin, Synthesis and in vitro evaluation of epidermal growth factor receptor tyrosine kinase inhibitors, *Journal of Nuclear Medicine* 39 (supplement), (1998) 20P–21P (abstract).

[18] E. Mishani, T.A. Bonasera, Y. Rozen, G. Ortu, A. Gazit, A. Levitzki, Fluorinated EGFr-TK Inhibitor-based Tracers for PET, *Journal of Labelled Compound and Radipharmaceuticals* 42 (Supplement 1 (conference abstracts)), (1999) S27–S29.

[19] E. Mishani, M.E. Cristel, C.S. Dence, T.J. McCarthy, M.J. Welch, Application of a novel phenylpiperazine formation reaction to the radiosynthesis of a model fluorine-18-labeled radiopharmaceutical (^{18}FTFMPP), *Nuclear Medicine and Biology* 24 (3) (1997) 269–273.

[20] G.K. Mulholland, W. Winkle, B.H. Mock, G. Sledge, Radioiodinated epidermal growth factor receptor ligands as tumor probes, Dramatic potentiation of binding to MDA-468 cancer cells in presence of EGF, *Journal of Nuclear Medicine* 36 (supplement) (1995) 71P.

[21] G.K. Mulholland, Q.-H. Zheng, W.L. Winkle, K.A. Carlson, Synthesis and biodistribution of new C-11 and F-18 labeled epidermal growth factor receptor ligands, *Journal of Nuclear Medicine*, 38 (supplement) (1997) 141P.

[22] M. Ramos-Suzarte, N. Rodriguez, J.P. Oliva, N. Iznaga-Escobar, A. Perera, A. Morales, N. Gonzalez, M. Cordero, L. Torres, G. Pimentel, M. Borrun, J. Gonzalez, O. Torres, T. Rodriguez, R. Perez, ^{99m}Tc-labeled antihuman epidermal growth factor receptor antibody in patients with tumors of epithelial origin: Part III. Clinical trials safety and diagnostic efficacy, *Journal of Nuclear Medicine* 40 (5) (1999) 768–775.

[23] G.W. Rewcastle, W.A. Denny, A.J. Bridges, H. Zhou, D.R. Cody, A. McMichael, D.W. Fry, Tyrosine kinase inhibitors, 5, Synthesis and structure-activity relationships for 4-[(phenylmethyl)amino]- and 4-(phenylamino)quinazolines as potent adenosine 5′-triphosphate binding site inhibitors of the tyrosine kinase domain of the epidermal growth factor receptor, *J. Med. Chem.* 38 (18) (1995) 3482–3487.

Elander, In vivo evaluation of the biodistribution of ^{11}C-labeled PD153035 in rats without and with neuroblastoma implants, *Life Sciences* 65 (2) (1999) 165–174.

[24] J.B. Smaill, B.D. Palmer, G.W. Rewcastle, W.A. Denny, D.J. Mc-Namara, E.M. Dobrusin, A.J. Bridges, H. Zhou, H.D. Showalter, R.T. Winters, W.R. Leopold, D.W. Fry, J.M. Nelson, V. Slintak, W.L. Elliot, B.J. Roberts, P.W. Vincent, S.J. Patmore, Tyrosine kinase inhibitors, 15, 4-(Phenylamino)quinazoline and 4-(phenylamino)py-rido[d]pyrimidine acrylamides as irreversible inhibitors of the ATP binding site of the epidermal growth factor receptor, *Journal of Medicinal Chemistry* 42 (10) (1999) 1803–1815.

[25] J.B. Smaill, G.W. Rewcastle, J.A. Loo, K.D. Greis, O.H. Chan, E.L. Reyner, E. Lipka, H.D. Showalter, P.W. Vincent, W.L. Elliott, W.A. Denny, Tyrosine kinase inhibitors, 17, Irreversible inhibitors of the epidermal growth factor receptor: 4-(phenylamino)quinazoline- and 4-(phenylamino)pyrido[3,2-d]pyrimidine-6-acrylamides bearing additional solubilizing functions, *Journal of Medicinal Chemistry* 43 (7) (2000) 1380–1397.

[26] S.E. Snyder, K.M. Whitmer, C. Brown-Procter, Synthesis of 3-chloro-4-[18F]fluoroaniline as a synthon for epidermal growth factor receptor inhibitors for tumor imaging with PET, *Journal of Labelled Compound and Radiopharmaceuticals* 42 (Supplement 1 (conference abstracts)) (1999) S522–S524.

[27] L. Vinter-Jensen, J. Frokiaer, P.E. Jorgensen, J. Marqversen, M. Rehling, E.Z. Dajani, E. Nexo, Tissue distribution of ^{131}I-labelled epidermal growth factor in the pig visualized by dynamic scintigraphy, *J. Endocrinol.* 144 (1) (1995) 5–12.

[28] Q. Zhao, V. Tolmachev, J. Carlsson, H. Lundqvist, J. Sundin, J.C. Janson, A. Sundin, Effects of dextranation on the pharmacokinetics of short peptides, A PET study on mEGF, *Bioconjug. Chem.* 10 (6) (1999) 938–946.